Title
Direct silver to aluminum solid-state bonding processes

Authors
Fu, Shao-Wei
Lee, Chin C

Publication Date
2018-04-01

DOI
10.1016/j.msea.2018.03.011

Peer reviewed

Materials Science & Engineering A 722 (2018) 160–166

Contents lists available at ScienceDirect

Materials Science & Engineering A

journal homepage: www.elsevier.com/locate/msea

Direct silver to aluminum solid-state bonding processes

Shao-Wei Fu*, Chin C. Lee

Electrical Engineering and Computer Science, Materials and Manufacturing Technology, University of California, Irvine, CA 92697-2660, USA

ARTICLE INFO

Keywords:
Silver-aluminum direct bonding
Solid-state bonding process
Intermetallic compound
Fracture mechanism
Electronic packaging

ABSTRACT

The high thermal conductivity, light weight, and low cost of aluminum (Al) make it a promising substrate material for high power electronic packaging. A main challenge of using aluminum in electronic packaging is its poor bondability. The native aluminum oxide (Al_2O_3) prevents aluminum from bonding to commonly used die-attach materials such as solders. Thus, zincating process is often needed to dissolve the Al_2O_3 layer and deposit a protective zinc layer which provides a basis for subsequent metallization or soldering processes.

In this research, Ag-Al solid-state bonding has been developed as a novel bonding technique to bond Ag directly to Al substrates. No surface treatment was applied on Al substrates to remove the native Al_2O_3 layer prior to bonding. The shear strength of Ag-Al joints passes the military criterion (MIL-STD-883H method 2019.8) by a large margin. SEM and TEM imaging was utilized to study the microstructures. In the bonding processes conducted at 425 and 450 °C, Ag and Al atoms inter-diffused through the thin Al_2O_3 to react and form Ag_2Al and Ag_3Al compounds. To examine the fracture modes of Ag-Al joints, the fracture surfaces after shear tests were evaluated. The effect of bonding temperatures on Ag-Al joint morphology and the fracture behaviors were investigated and discussed.

An application of this new technique is to bond thin Ag foils to Al substrates and make them bondable to die-attach materials such as solders and nano-silver paste. This Ag foil bonding method provides an alternative to the zincating process. Other potential applications include making Al surfaces easier to blaze to other metals such as brass, bronze and copper.

1. Introduction

In recent years, high temperature electronic packaging has been rapidly developed due to increasing demand of power electronics applications, particularly for the automotive, aerospace, and energy production industries [1–3]. The introduction of silicon carbide and gallium nitride semiconductors has enabled power electronics to operate at high temperatures above 350 °C [4]. For continuous operations under extreme high temperatures, novel interconnection materials and packaging structures are required for power electronics systems [5,6].

Direct bond copper (DBC) substrates have been widely used in power electronics for many years [7,8]. DBC substrates have advantages of high current carrying capacity, relatively high thermal conductivity, and controlled coefficient of thermal expansion (CTE) [9]. Recently, reliability issues of DBC substrates in thermal cycling tests have been reported [10–12]. The thermal cycling stress induces cracks at the copper/ceramic interface, leading to the eventual delamination of DBC substrates [10,11]. As a possible alternative, direct bond aluminum (DBA) substrates have been developed [13,14]. DBA substrates outperform DBC substrates in thermal cycling tests [14,15]. The reason is the lower yield stress and plastic strain rate of aluminum as opposed to copper, which result in lower thermomechanical stress at the aluminum/ceramic interface and less strain hardening during thermal cycling. No crack or delamination was observed in DBA substrates after 1500 thermal cycles from −55 °C to 250 °C [15].

A main challenge of using aluminum layers or substrates in electronic packaging is its poor bondability. The native aluminum oxide layer prevents aluminum from electroless or electrolytic plating of metallization layer, which is an essential step to make aluminum bondable to die-attach materials such as solders and nano-silver paste [16]. Thus, the zincating process is required to prepare DBA substrates for further metallization processing. During the zincating process, the aluminum oxide is dissolved in the zincating solution, and a layer of zinc is deposited to protect the surface, providing a basis for subsequent metallization [17]. The zincating process exhibits a narrow process window due to its high reaction sensitivity to aluminum surface conditions [18,19]. The zincating and following metallization processes on aluminum largely increase the processing cost and add more reliability issues [20].

In this research, Ag-Al solid-state bonding has been developed as a

* Corresponding author.
E-mail address: shaoweif@uci.edu (S.-W. Fu).

https://doi.org/10.1016/j.msea.2018.03.011
Received 29 November 2017; Received in revised form 1 March 2018; Accepted 2 March 2018
Available online 04 March 2018
0921-5093/

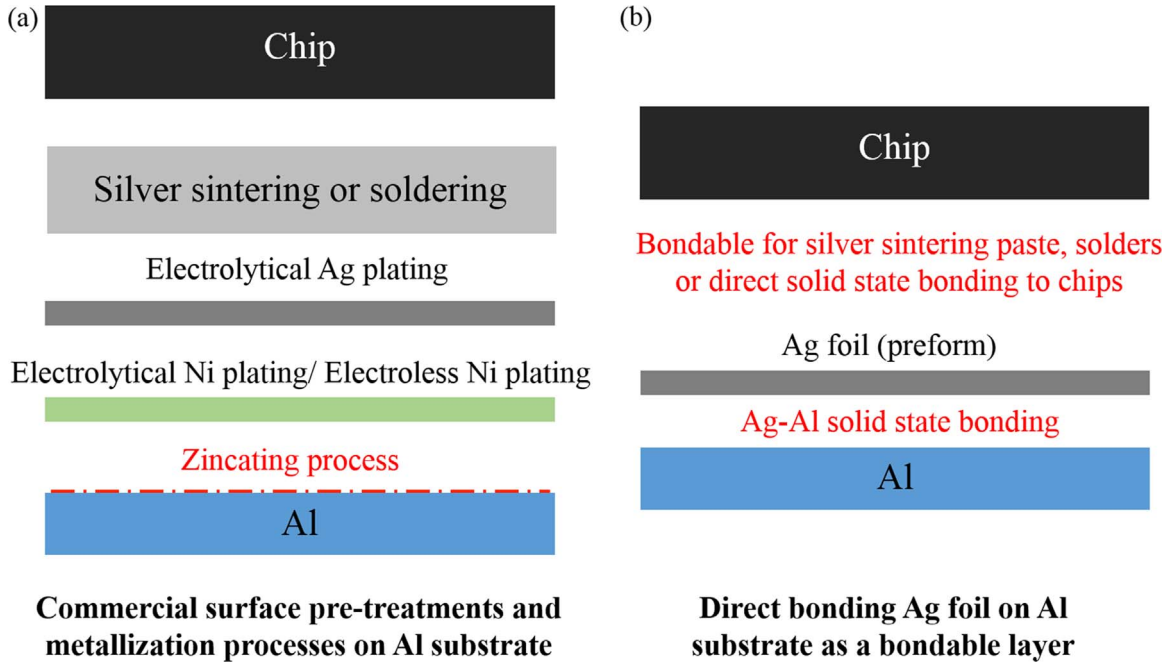

Fig. 1. (a) Commercial surface pre-treatments and metallization processes on Al substrate in electronic packaging. (b) Proposed Ag-Al solid-state bonding technique to direct bond Al foil on Al substrate as a bondable layer which is compatible with nano-silver paste and solders. In a more advanced level, device chips can be bonded to the Ag foil on Al substrates at 300 °C using solid-state bonding technique.

novel bonding technique to directly bond Ag to Al substrates. SEM and TEM analyses were utilized to study the microstructures and fracture mechanisms. In the solid-state bonding process at 425 and 450 °C, Ag and Al atoms inter-diffused through the thin aluminum oxide layer to react and form Ag_2Al and Ag_3Al. The shear strength of the Ag-Al joints passes the military criterion with a large margin. As shown in Fig. 1, an application of this new technique is to bond Ag foils to Al substrates and make them bondable to solders and nano-silver paste. This foil bonding technique provides an alternative to the zincating and metallization processes on aluminum substrates. At a more advanced level, device chips can be bonded to Al substrates using Ag foils as the bonding medium at 300 °C.

2. Experimental design and procedures

To achieve Ag-Al solid-state bonding, Ag disks (10 mm in diameter and 1 mm in thickness) and Al substrates (15 mm × 12 mm × 1 mm) with 99.9% purity are employed. Ag disks were grown through the ingot casting method followed by annealing [21,22]. Ag shots with 99.99% purity were loaded into 150 mm long quartz tubes with 10 mm in inner diameter. After loading, the tubes were evacuated by a vacuum pump and sealed by a hydrogen torch to form capsules. The capsules were brought to and kept at 1000 °C for 2 h, followed by 48-h annealing at 850 °C to ensure complete homogenization. After annealing, the ingots (50 mm long and 10 mm in diameter) were cut into disks with a thickness of 1.5 mm. Ag disks and Al substrates were ground with silicon carbide-coated papers up to 2000 grits and polished with 1 μm diamond powder suspended fluid to achieve clean surfaces for bonding. During the bonding process, the Ag disk is placed over the Al substrate and held by a fixture with 1000 psi (6.89 MPa) static pressure to ensure intimate contact. The assembly is loaded on a graphite platform in a vacuum furnace and heated with temperature monitored by a miniature thermocouple. The solid-state bonding is performed at a vacuum level of 0.1 Torr (13.33 Pa) to suppress oxidation. The bonding temperatures are selected as 400 °C, 425 °C, and 450 °C, respectively, with a bonding time of 10 min.

The microstructures and phase compositions of the resulting Ag-Al joints are examined using scanning electron microscopy/energy dispersive X-ray spectroscopy (SEM/EDX, FEI Philips XL-30, FEG SEM) in back-scattered electron (BSE) mode. The standard single-strap-joint configuration [23,24] was used to evaluate the shear strength of the Ag-Al joints. The shear test was conducted at room temperature using a tensile testing machine (Model 8800, Instron Corporation) with a crosshead speed of 1 mm/minute. After the shear test, the fracture surfaces of the joints are evaluated. The phase compositions of the fracture surface are probed by SEM/EDX and X-ray diffraction (XRD). The area ratios of the fractured phases are analyzed using ImageJ software. To further investigate the phase distribution at the Ag/Al interface and the failure mechanism of the Ag-Al joint, transmission electron microscopy (TEM) analysis is conducted with a model JEOL-2100F equipped for scanning TEM (STEM) [25]. The TEM specimens are prepared with an in-situ method of dual-beam focused ion beam (FIB) on Tescan GAIA3 SEM/FIB.

3. Experimental results and discussions

In experiments, Ag disks, produced in house, were bonded to Al substrates using solid-state bonding technique without any flux or interlayer. Fig. 2 shows cross-section back-scattered electron images of Ag-Al joints bonded at 400 °C, 425 °C, and 450 °C, respectively, for 10 min. For the Ag-Al joint bonded at 400 °C, Fig. 2(a), no intermetallic compound (IMC) formation was observed. During solid-state bonding, Ag and Al conformed to each other through elastic deformation to achieve intimate contact on the interface. On the bonding interface, no cracks or voids were observed. As the bonding temperature was raised above 425 °C, Ag-Al IMC formed at the bonding interface, as exhibited in Fig. 2(b) and (c). With 425 °C bonding temperature, the microstructure reveals island-like IMC. With 450 °C bonding temperature, a continuous IMC layer was produced. These results indicate that the IMC morphology and growth are strongly dependent on the bonding temperature. In solid-state bonding process, higher bonding temperature accelerates interdiffusion of Ag and Al and thus enhances IMC growth. The SEM images at higher magnification show the IMC grew into both Al and Ag regions away from the bonding interface. A thin black line was observed. This line was later identified as the aluminum oxide (Al_2O_3) layer on the Al substrate before bonding. Thus, this line can act

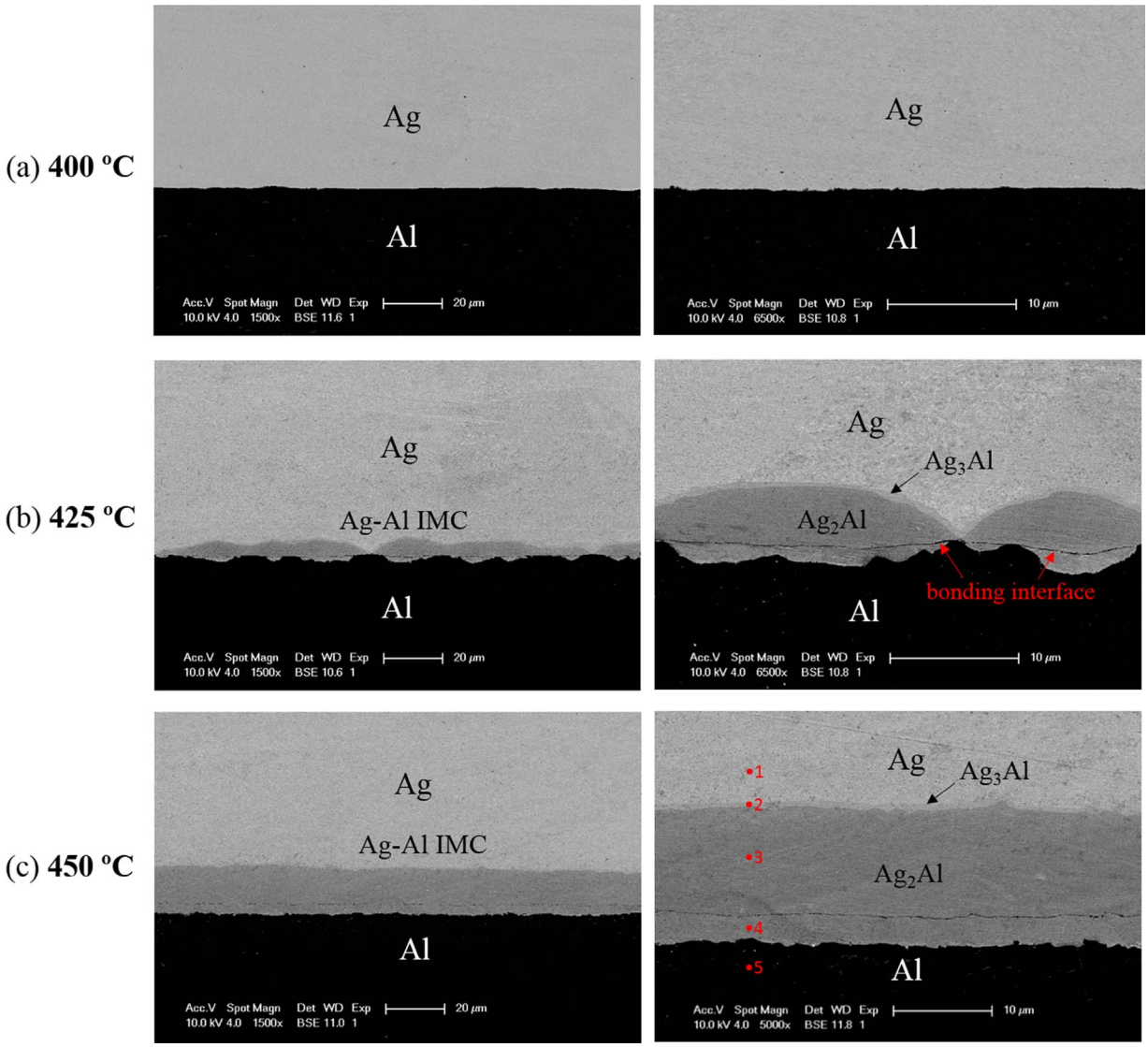

Fig. 2. SEM back-scattered electron images of Ag-Al joints bonded at (a) 400 °C, (b) 425 °C, and (c) 450 °C for 10 min. In the enlarged image of (c), the red dots marked by 1–5 indicate the EDX analysis locations and the resulting element compositions are listed in the Table 1. (For interpretation of the references to color in this figure legend, the reader is referred to the web version of this article.)

Table 1
EDX data on locations 1 − 5 near Ag-Al interface in Fig. 2(c).

Locations	Ag (at%)	Al (at%)	Phases
1	98.7	1.3	(Ag)
2	77.9	22.1	Ag_3Al
3	65.7	34.3	Ag_2Al
4	65.5	34.5	Ag_2Al
5	0.8	99.2	(Al)

as a marker of the original Ag-Al contact interface. EDX analysis was performed on the enlarged SEM image, Fig. 2(c), where red dots marked 1 − 5 indicate locations at which the resulting compositions are listed in Table 1. Based on the EDX data, the IMC growing into the Al region is identified as Ag_2Al. The IMC phases growing into the Ag region were characterized as Ag_2Al and Ag_3Al, where the Ag_3Al layer is very thin and between the Ag_2Al and Ag regions. As indicated in Table 1, the compositions of Ag_2Al on locations 3 and 4 are approximately 34.5 at% Al while the thin Ag_3Al layer contains 22.1 at% Al. The Ag-Al phase diagram is presented in Fig. 3 to show the composition ranges of the Ag_2Al and Ag_3Al intermetallic phases [26].

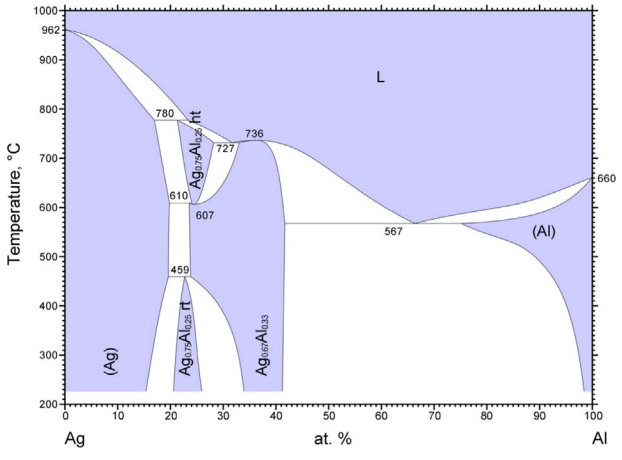

Fig. 3. Ag-Al binary phase diagram [26].

The shear strength of the Ag-Al joints was evaluated by standard single-strap-joint shear test [23]. The specimens were tested at room temperature using a tensile testing machine with a crosshead speed of

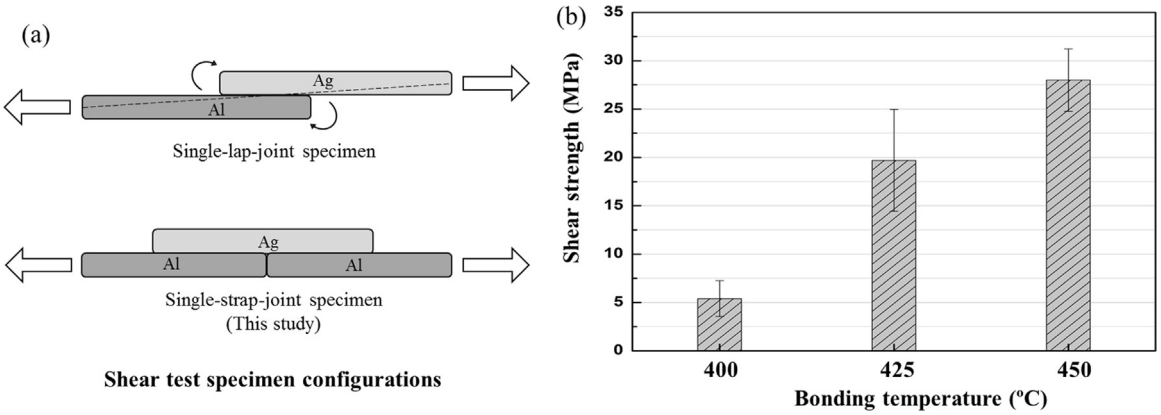

Fig. 4. (a) The schematic diagram of the shear test specimen configurations: single-lap-joint and single-strap-joint (used in this study). (b) The shear strength of the Ag-Al joints bonded at 400 °C, 425 °C, and 450 °C, respectively.

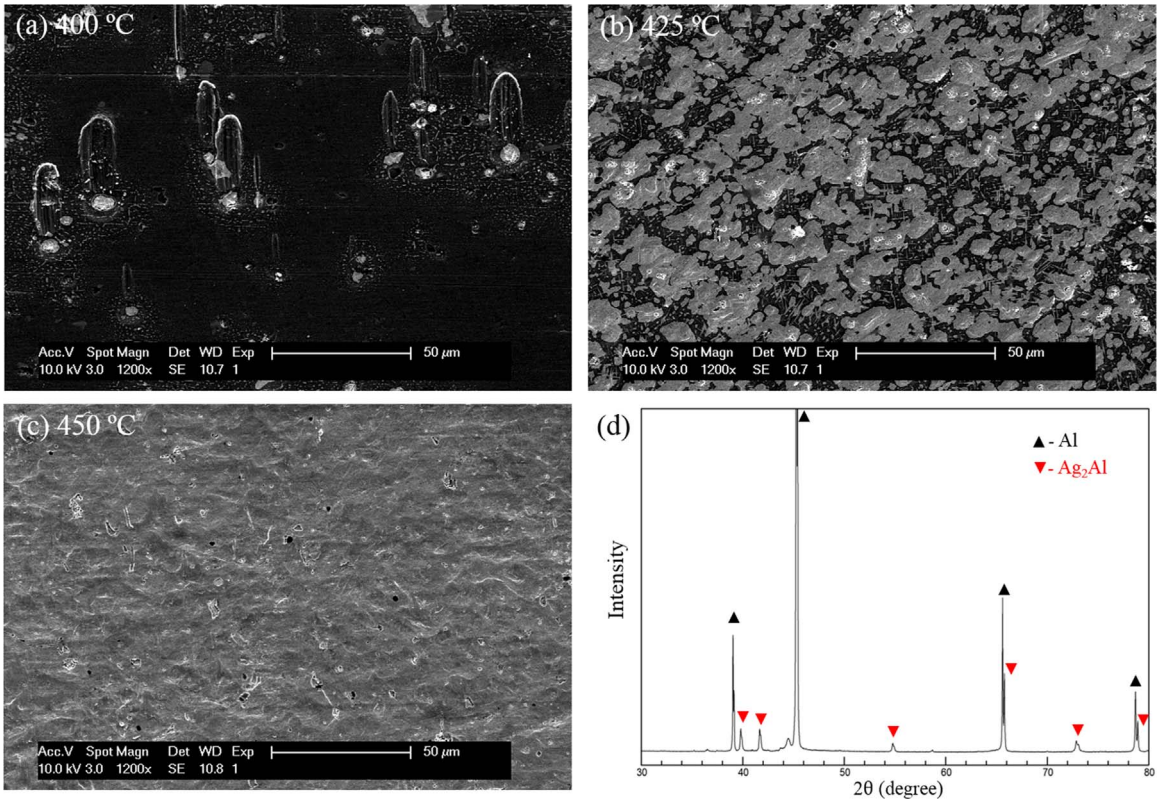

Fig. 5. SEM back-scattered images of the fracture surfaces on the Al side of the Ag-Al joints bonded at (a) 400 °C, (b) 425 °C, and (c) 450 °C. The XRD spectrum of the fracture surface on the Al side of the Ag-Al joints bonded at 450 °C is presented in (d).

1 mm/minute. The single-lap-joint and single-strap-joint specimen configurations are illustrated in Fig. 4(a). In the typical single-lap-joint shear test, the shear strength and fracture behavior could be influenced by the non-uniform stress distribution along the bonded region [27]. In this study, to minimize the normal stress created by the bending moment on the shear test sample [28], the single-strap-joint was chosen as the shear test configuration. Fig. 4(b) shows the shear strength of the joints bonded at temperatures of 400 °C, 425 °C, and 450 °C, respectively. Test results show that the Ag-Al joints bonded at 450 °C exhibit the highest shear strength of 28.0 MPa. For samples bonded at 425 °C and 400 °C, shear strength values of 19.7 MPa and 5.4 MPa, respectively, were obtained. The standard deviations of the joint shear strength of each bonding condition are also shown in Fig. 4(b). These joint strength values pass the military criterion (MIL-STD-883H method 2019.8) by a large margin [29]. To understand the fracture behavior of the Ag-Al joints, the fracture surfaces after the shear test were studied. The phase compositions were probed by SEM/EDX and XRD. The area ratios of fracture phases were analyzed using ImageJ software. Fig. 5 shows the SEM micrographs of the fracture surfaces on the Al side of the Ag-Al joints. In the sample bonded at 400 °C, the fracture surface clearly shows 94% Al and only 6% Ag_2Al. No Ag traces are observed on the Al regions, indicating weak bonding interface between the Ag disk and Al substrate. For the sample bonded at 425 °C, the microstructure exhibits a mixture of Ag_2Al and Al. The Ag_2Al regions significantly increased up to 71% of the total fracture area. For the sample bonded at 450 °C, the fracture surface is 100% Ag_2Al, indicating that the breakage incurs within the continuous Ag_2Al layer. The XRD spectrum on the fracture surface of the Al side of the Ag-Al joints bonded at 450 °C is presented in Fig. 5(d). The XRD pattern reveals the presence of Ag_2Al and Al. Since Ag_2Al layer thickness is much smaller than the X-ray penetration depth,

Table 2
The shear strength and the fracture surface composition of Ag-Al joints bonded at 400 °C, 425 °C, and 450 °C, respectively.

Bonding temperature	Shear strength	Composition on fracture surface
400 °C	5.4 MPa	94% Al and 6% Ag_2Al
425 °C	19.7 MPa	29% Al and 71% Ag_2Al
450 °C	28.0 MPa	100% Ag_2Al

the strong Al peaks were caused by the Al substrate beneath the Ag_2Al layer. The shear strength of the Ag-Al joints and the phase distribution on the fracture surfaces are summarized in Table 2. Experimental results show that the shear strength of Ag-Al solid-state bonding are related to the area of intermetallic compound formation. With little IMC formation, the samples bonded at 400 °C exhibits relatively weak bonding and the joint fracture along the Ag/Al interface. A thin Al_2O_3 layer exists at the Ag/Al interface, as will be shown in next paragraph. This Al_2O_3 layer prevents Ag atoms to get into intimate contact with Al atoms. For the samples bonded at higher temperatures of 425 °C and 450 °C, Ag and Al atoms are able to inter-diffuse through the thin Al_2O_3 layer to react and form Ag_2Al regions. With a continuous Ag_2Al layer through the joint interface, the sample bonded at 450 °C exhibits the highest shear strength.

To further investigate exactly where the joint bonded at 450 °C fractured within the Ag_2Al region, the Ag side and Al side of the sample after shear test were molded with epoxy, cut in cross sections and polished for characterization. Fig. 6 shows the back-scattered electron images of the fractured Ag-Al joints. It is clearly observed that the fracture occurred along the black line shown in Fig. 2(c), and a thin Ag_2Al layer, which was originally beneath the black line, was left on the Al substrate. Also, isolated micro-cracks within the thin Ag_3Al layer were observed, shown in Fig. 6(c) and (d). The micro-cracks were confined within the Ag_3Al layer and did not propagate into Ag_2Al or Ag region. No cracks were seen within the Ag_2Al, indicating that Ag_2Al is relatively ductile compared to Ag_3Al. In this study, no surface pretreatment was applied on the Al substrates to remove the native oxide layer before the solid-state bonding process. It is probable that the thin black line is attributed to the native Al_2O_3 on Al substrates prior to bonding. In the solid-state bonding process at elevated temperatures, Ag and Al atoms inter-diffused through the thin Al_2O_3 layer to react and form Ag_2Al layer. As seen in Fig. 2(b), the initial Ag_2Al growth was non-uniform along the bonding interface. Initial growth began on the bonding interface regions where Ag atoms and Al_2O_3 molecules had atomic contact. The thin Al_2O_3 layer had nowhere to go and thus was embedded within the resulting the Al_2Al layer. In the following section, nano-structures were studied in details using TEM and STEM with electron diffraction technique to confirm that the black line is indeed composed of Al_2O_3 within Ag_2Al region.

Figs. 7 and 8 show the TEM images on the bonding interface cross section of a Ag-Al joint bonded at 450 °C. The TEM specimens were prepared using in-situ dual focused ion beams in an SEM (Tescan GAIA3). The ion-milled region is denoted by the red rectangle on the SEM image, Fig. 7(a). The scanning TEM images reveal $Ag_2Al/Al_2O_3/Ag_2Al/Al$ structure. The Al_2O_3 layer is clearly observed in Fig. 7(b), pointed out by red arrows. Fig. 8 displays high resolution STEM images of the Ag_2Al/Al interface region and a Ag_2Al region with embedded Al_2O_3 layer. Report shows that the transition temperature of amorphous Al_2O_3 to transform into γ-Al_2O_3 is about 550 °C [30]. In this research, the amorphous Al_2O_3 grew extremely slowly and remained stable during the solid-state bonding process at 450 °C. As shown in Fig. 8(b), the Al_2O_3 layer is 5 nm in thickness, continuous, and well connected to enclosing Ag_2Al at atomic level without any nano-voids or nano-cracks. The selected area diffraction patterns (SADP) of encircled zones in Fig. 8 are displayed in the inserts. The SADP patterns confirm the selected area to be Ag_2Al with hexagonal crystal structure, space group: *P*63/*mmc*, and a = b = 2.887 Å, c = 4.624 Å, as characterized along [11 $\bar{2}$ 1] zone axis. Furthermore, it is worth pointing out that no silver oxide (Ag_2O) was observed at the Ag-Al bonding interface, since Ag_2O

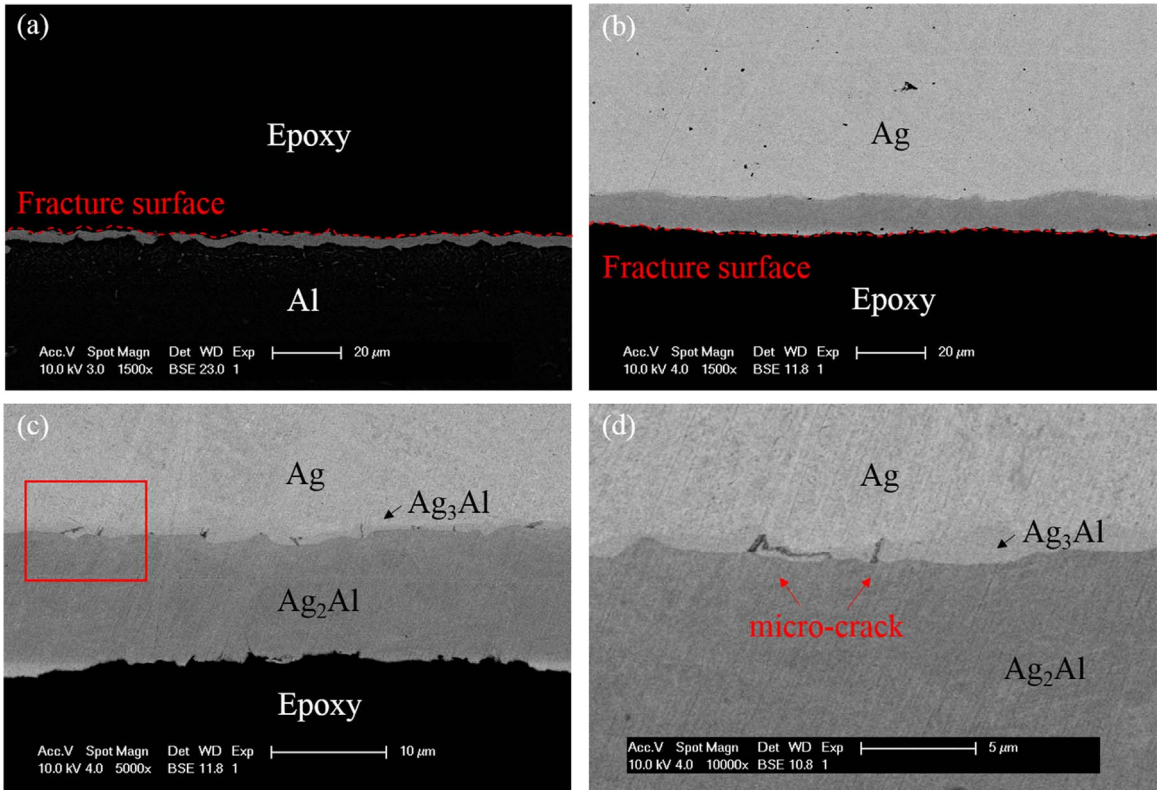

Fig. 6. SEM back-scattered images on the cross-sections of Ag-Al joint bonded at 450 °C after shear test (a) Al side and (b) Ag side. Enlarged SEM images on the Ag side are presented in (c) and (d).

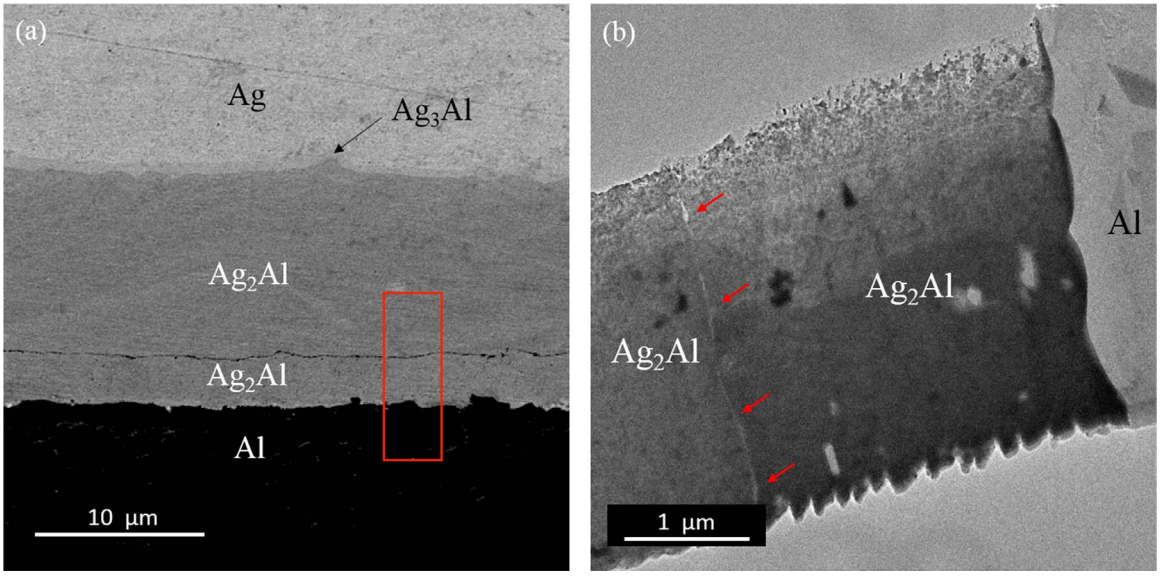

Fig. 7. (a) The SEM cross section image showing the interface region of a Ag-Al joint bonded at 450 °C. (b) The TEM image of the rectangle box in (a), where aluminum oxide line is indicated by red arrows. The TEM specimen was prepared by in-situ dual focused ion beams (FIB).

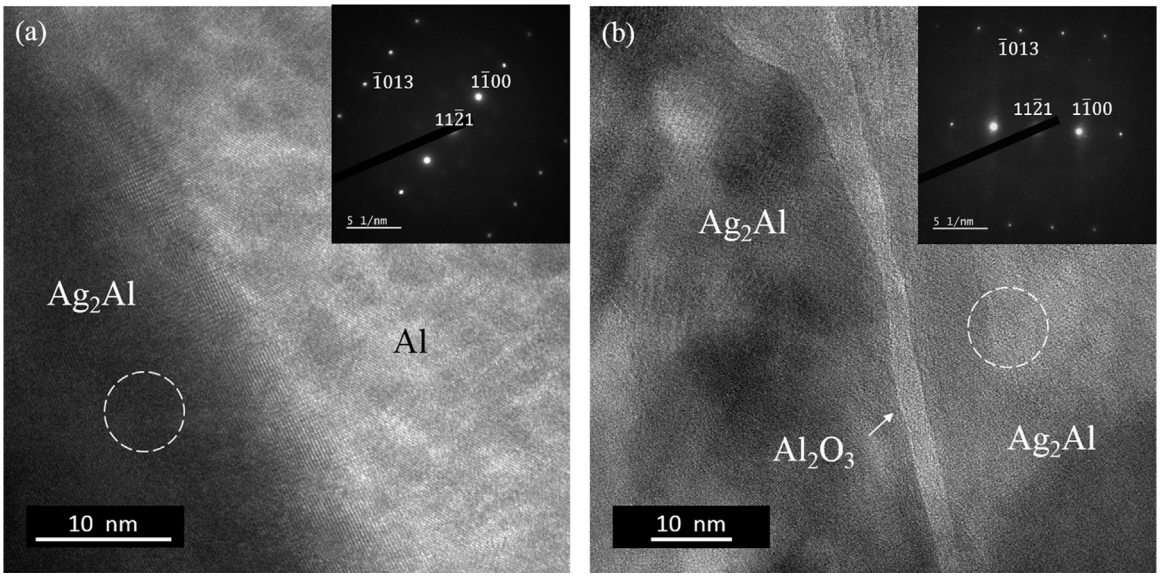

Fig. 8. High resolution STEM images of (a) the Ag_2Al/Al interface region and (b) a Ag_2Al region containing a thin Al_2O_3 layer. The inserts display selected area diffraction patterns (SADP) of the encircled Ag_2Al zones characterized along [11 $\bar{2}$ 1] zone axis.

is thermodynamically unstable at high temperature (> 220 °C) and tends to decompose in vacuum at 118–220 °C [31,32].

4. Summary

In this research, Ag-Al solid-state bonding was achieved at 400, 425, and 450 °C, respectively, to bond Ag directly to Al substrates. This bonding was deemed not possible in the past because of the native oxide on the Al substrate. Our experimental results, however, show that this bonding is achievable so far as the Ag and Al atoms on the interface can interdiffuse through the thin Al_2O_3 layer. No surface treatment was applied on Al substrates to remove the native Al_2O_3 layer before the bonding. Microstructures of the resulting Ag-Al joints were evaluated by SEM and TEM. For the samples bonded at 425 and 450 °C, the results clearly show that Ag and Al atoms indeed inter-diffused through the thin Al_2O_3 layer to react and form Ag_2Al and Ag_3Al compounds. Using STEM imaging, 5 nm thick Al_2O_3 layer was observed within the Ag_2Al region. It seems that the embedded Al_2O_3 layer was well connected to Ag_2Al region at atomic level. The shear strength of the Ag-Al joints passes the military criterion, MIL-STD-883H method 2019.8, by a large margin. Fracture analyses show that fracture occurred within the Ag_2Al region and extended along the bonding interface. This new Ag-Al bonding process is valuable in opening up more and new Al application as platforms or substrates by bonding a thin Ag layer at selected areas to make them bondable or solder-able.

Acknowledgments

SEM/EDX, TEM, and XRD analysis were performed at the UC Irvine Materials Research Institute (IMRI). The shear test was conducted with the assistance of Prof. Enrique Lavernia's group in Department of Chemical Engineering and Materials Science at University of California, Irvine.

References

[1] C. Buttay, D. Planson, B. Allard, D. Bergogne, P. Bevilacqua, C. Joubert, M. Lazar, C. Martin, H. Morel, D. Tournier, State of the art of high temperature power electronics, Mater. Sci. Eng.: B 176 (4) (2011) 283–288.

[2] P. Hagler, P. Henson, R.W. Johnson, Packaging technology for electronic applications in harsh high-temperature environments, IEEE Trans. Ind. Electron. 58 (7) (2011) 2673–2682.

[3] A. Lostetter, F. Barlow, A. Elshabini, An overview to integrated power module design for high power electronics packaging, Microelectron. Reliab. 40 (3) (2000) 365–379.

[4] P.G. Neudeck, R.S. Okojie, L. Chen, High-temperature electronics-a role for wide bandgap semiconductors? Proc. IEEE 90 (6) (2002) 1065–1076.

[5] L. Coppola, D. Huff, F. Wang, R. Burgos, D. Boroyevich, "Survey on high-temperature packaging materials for SiC-based power electronics modules," in: Proceedings of the Power Electronics Specialists Conference, 2007. PESC 2007. IEEE, 2007, pp. 2234–2240.

[6] M.R. Werner, W.R. Fahrner, Review on materials, microsensors, systems and devices for high-temperature and harsh-environment applications, IEEE Trans. Ind. Electron. 48 (2) (2001) 249–257.

[7] H. He, R. Fu, D. Wang, X. Song, M. Jing, A new method for preparation of direct bonding copper substrate on Al_2O_3, Mater. Lett. 61 (19) (2007) 4131–4133.

[8] B. Mouawad, B. Thollin, C. Buttay, L. Dupont, V. Bley, D. Fabregue, M. Soueidan, B. Schlegel, J. Pezard, J. Crebier, Direct copper bonding for power interconnects: design, manufacturing, and test, IEEE Trans. Compon., Packag. Manuf. Technol. 5 (1) (2015) 143–150.

[9] J. Schulz-Harder, Advantages and new development of direct bonded copper substrates, Microelectron. Reliab. 43 (3) (2003) 359–365.

[10] Y. Yoshino, H. Ohtsu, T. Shibata, Thermally induced failure of copper-bonded alumina substrates for electronic packaging, J. Am. Ceram. Soc. 75 (12) (1992) 3353–3357.

[11] G. Dong, X. Chen, X. Zhang, K.D. Ngo, G. Lu, Thermal fatigue behaviour of Al_2O_3-DBC substrates under high temperature cyclic loading, Solder. Surf. Mt. Technol. 22 (2) (2010) 43–48.

[12] D. Camilleri, Thermo-mechanical behaviour of DBC substrate assemblies subject to soldering fabrication processes, Solder. Surf. Mt. Technol. 24 (2) (2012) 100–111.

[13] S. Kraft, A. Schletz, M. Maerz, "Reliability of silver sintering on DBC and DBA substrates for power electronic applications," in: Proceedings of the Integrated Power Electronics Systems (CIPS) 7th International Conference on, 2012, pp. 1–6.

[14] D.C. Katsis, Y. Zheng, "Development of an extreme temperature range silicon carbide power module for aerospace applications," in: Proceedings of the Power Electronics Specialists Conference, 2008. PESC 2008. IEEE, 2008, pp. 290–294.

[15] T.G. Lei, J.N. Calata, K.D. Ngo, G. Lu, Effects of large-temperature cycling range on direct bond aluminum substrate, IEEE Trans. Device Mater. Reliab. 9 (4) (2009) 563–568.

[16] S. Lee, J. Lee, Y. Kim, Nucleation and growth of zinc particles on an aluminum substrate in a zincate process, J. Electron Mater. 36 (11) (2007) 1442–1447.

[17] M.M. Arshad, I. Ahmad, A. Jalar, G. Omar, U. Hashim, The effects of multiple zincation process on aluminum bond pad surface for electroless nickel immersion gold deposition, J. Electron. Packag. 128 (3) (2006) 246–250.

[18] K. Azumi, S. Egoshi, S. Kawashima, Y. Koyama, Effect of copper pretreatment on the double zincate process of aluminum alloy films, J. Electrochem. Soc. 154 (4) (2007) D220–D226.

[19] J. Lee, I. Lee, T. Kang, N. Kim, S. Oh, The effects of bath composition on the morphologies of electroless nickel under-bump metallurgy on Al input/output pad, J. Electron. Mater. 34 (1) (2005) 12–18.

[20] S. Robertson, I. Ritchie, The role of iron (III) and tartrate in the zincate immersion process for plating aluminium, J. Appl. Electrochem. 27 (7) (1997) 799–804.

[21] S. Fu, C.C. Lee, A study on intermetallic compound formation in Ag-Al system and evaluation of its mechanical properties by micro-indentation, J. Mater. Sci.: Mater. Electron. 29 (5) (2018) 3985–3991.

[22] S. Fu, C.C. Lee, A corrosion study of Ag–Al intermetallic compounds in chlorine-containing epoxy molding compounds, J. Mater. Sci.: Mater. Electron. 28 (20) (2017) 15739–15747.

[23] S.S. Smeltzer, Testing of structural joints, Encycl. Aerosp. Eng. (2010).

[24] L. Tong, J. Spelt, G. Fernlund, Strength determination of adhesive bonded joints, in: L. Tong, C. Soutis (Eds.), Recent Advances in Structural Joints and Repairs for Composite Materials, Springer, 2003, pp. 27–66.

[25] ⟨https://www.aphys.kth.se/polopoly_fs/1.190438!/Menu/general/column-content/attachment/TEM_manual_JEOL2100.pdf⟩.

[26] S. Lim, P. Rossiter, J. Tibballs, Assessment of the al-ag binary phase diagram, Calphad 19 (2) (1995) 131–141.

[27] D. Oplinger, Effects of adherend deflections in single lap joints, Int. J. Solids Struct. 31 (18) (1994) 2565–2587.

[28] L. Hart-Smith, Designing to minimize peel stresses in adhesive-bonded joints, Delamination and Debonding of Materials, ASTM International, 1985.

[29] Department of Defense, U.S.A., Test Method Standard Microcircuits, 2010, MIL-STD-883H method 2019.8.

[30] M.A. Trunov, M. Schoenitz, E.L. Dreizin, Effect of polymorphic phase transformations in alumina layer on ignition of aluminium particles, Combust. Theory Model. 10 (4) (2006) 603–623.

[31] W. Garner, L. Reeves, The thermal decomposition of silver oxide, Trans. Faraday Soc. 50 (1954) 254–260.

[32] B.V. L'vov, Kinetics and mechanism of thermal decomposition of silver oxide, Thermochim. Acta 333 (1) (1999) 13–19.